Nonlinear Multi-Physics Coupling for Non-Conforming Interfaces based on a Dual Mortar Formulation

By J. Westfall†, K. K. Maute†, T. Klöppel‡, A. Popp‡, M. Gitterle‡ AND W. A. Wall‡

†Center for Aerospace Structures, University of Colorado at Boulder
‡Institute for Computational Mechanics, Technische Universität München

In the present work, the problem of coupling multiple physical phenomenon in a finite element framework with an interface between two or more non-conforming meshes is considered. Recently the research group at the Institute for Computational Mechanics, Technische Universität München has developed a dual mortar method of monolithic coupling for fluid structure interactions (FSI) involving incompressible fluid. The research group at the Center for Aerospace Structures, University of Colorado at Boulder has developed a residual based method of monolithic coupling that includes FSI, as well as fluid thermal coupling including nonlinear surface effects such as ablation. Both methods take advantage of the benefits of solving a monolithic system which is of the same size as the uncoupled system and does not include Lagrange multipliers in the final system. One of the primary benefits of this is the ability to use well developed iterative linear solvers. The goal of this summer research is to combine the capabilities of both research groups so as to extend the dual mortar method to include compressible FSI problems and fluid thermal interactions with nonlinear surface affects.

1. Introduction

The numerical simulation of multi-physics phenomena is of particular interest in high speed aerodynamic applications. High speed flow environments such as supersonic aircraft and re-entry vehicles can have complex aerodynamic flows, significant thermal heating, to include phase change and chemical ablation, as well as important elasto-dynamic responses. There are several possible solution strategies to solve these tightly coupled physics, including weakly coupled partitioned, strongly coupled partitioned, and monolithic schemes. Partitioned schemes allow for the use of established field solvers and are hence relatively simple to implement. However, in the context of shape and topology optimization for aerodynamic problems, monolithic schemes make efficient sensitivity analysis possible by taking advantage of a single discretization method and one time integrator for all equations.

In general and also in [1], monolithic schemes are derived based on the assumption of a conforming interface discretization, i.e. fluid and structure share a common interface mesh. In these cases, enforcement of coupling conditions is straightforward, as in the residual based method used by the group from University of Colorado. There are many cases that one would like to deal with non-matching grids at the fluid-structure interface. Most often different resolution requirements in the different physical domains or quite

simply the presence of complex interface geometries make the creation of matching fluid and structure meshes cumbersome or even impossible.

A possible remedy is provided by the mortar method, which has originally been introduced in the context of non-overlapping domain decomposition [2]. A characteristic feature of the mortar method is the imposition of interface constraints in a variationally consistent manner based on Lagrange multipliers. This approach has seen a great thrust of research over the past decade. New fields of application such as finite deformation contact analysis [3–7] have been established and the mathematical understanding concerning the choice of adequate discrete Lagrange multiplier spaces has been deepened [8–11].

To overcome the numerical issues of the standard mortar method discussed above for both partitioned and monolithic coupling schemes, the research group from Technische Universität München has employed a so-called dual mortar method [8–12] with discrete Lagrange multipliers that are constructed based on a bi-orthogonality relation with the primal shape functions at the fluid-structure interface. In contrast to standard mortar methods, the dual mortar approach allows for an elimination of the additional degrees of freedom by condensation at negligible computational cost in the monolithic setting. This ensures that there are only non-zero diagonal entries in the global system matrix and hence the applicability of efficient iterative solvers.

The goal of the collaboration on this research is to extend the dual mortar method developed by Prof. Wall's research group to include compressible flow, fluid-thermal interactions, and non-linear surface effects such as wear and ablation. Currently the dual mortar method is implemented for only incompressible flows. This is more straight forward as the flow field is solved for unknown velocities which have a linear relationship to the structural displacements. For compressible flow, formulated in conservative form, density, momentum, and density times total energy are the unknowns, making for a nonlinear relationship between the structural temperature and the fluid unknowns as well as the structural displacements and the fluid unknowns.

The remainder of this article is organized as follows: The next section briefly introduces the governing equations as well as the weak forms. In Sec. 3 the dual mortar method is explained in detail in the context of incompressible FSI problems, starting with the discretization in space and time. The obtained nonlinear equations are linearized. The last part of this section introduces the resulting monolithic system of equations. The condensed linear monolithic systems are deduced in Sec. 4 depending on the choice of master and slave discretization at the interface. In both cases the field of Lagrange multipliers is eliminated from the system.

2. Problem definition

Fluid, structure, and thermal interaction problems can formally be described as seven field problems. There are three physical fields, fluid, structure and temperature. To account for deformations of the fluid field, an arbitrary Lagrangian-Eulerian (ALE) approach is employed, constituting a fourth, non-physical mesh field later also called ALE field. The thermal and/or structural field can have similar deformations due to non-linear surface effects such as ablation or wear and therefore an additional fifth non-physical ALE field for the thermal/structural field is used. Fluid-structure and fluid-thermal share a common interface Γ, but not necessarily a common finite element discretization of this interface. Therefore, coupling conditions are applied in a weak sense, which introduces

two more fields of Lagrange multipliers λ at Γ, one each for structural coupling and thermal coupling.

In this section we briefly present the governing equations of the fluid field defined on a deformable domain, the structure field and the thermal field defined on a deformable domain. The additional terms due to the weak coupling of the fields at the interface are also discussed.

In the following, fluid quantities are denoted by the superscript $\cdot^{\mathrm{F}}$, quantities of the mesh (or grid) field by $\cdot^{\mathrm{G}}$, and finally those of the structure field by $\cdot^{\mathrm{S}}$.

2.1. *Fluid*

The present work is to extend the dual mortar method to include compressible Navier-Stokes equations for a Newtonian fluid on a deformable fluid domain Ω^{F}. The unknown fluid domain deformation $\mathbf{d}^{\mathrm{G}}$ is defined by a unique mapping $\boldsymbol{\varphi}$ given by

$$\mathbf{d}^{\mathrm{G}}(\mathbf{x},t) = \boldsymbol{\varphi}\left(\mathbf{d}_{\Gamma}^{\mathrm{G}}, \mathbf{x}, t\right) \quad \text{in} \quad \Omega^{\mathrm{F}} \times (0, t_f), \tag{2.1}$$

based on the mesh interface displacement $\mathbf{d}_{\Gamma}^{\mathrm{G}}$, that will later be related to the structure interface displacement $\mathbf{d}_{\Gamma}^{\mathrm{S}}$. This mapping (2.1) is arbitrary and defines the domain velocity $\mathbf{u}^{\mathrm{G}}$ by

$$\mathbf{u}^{\mathrm{G}} = \frac{\partial \boldsymbol{\varphi}}{\partial t} \quad \text{in} \quad \Omega^{\mathrm{F}} \times (0, t_f), \tag{2.2}$$

which has to match the fluid velocity $\mathbf{u}_{\Gamma}^{\mathrm{F}}$ at the interface Γ, i.e.

$$\mathbf{u}_{\Gamma}^{\mathrm{F}} = \mathbf{u}_{\Gamma}^{\mathrm{G}} \quad \text{in} \quad \Gamma \times (0, t_f). \tag{2.3}$$

Equation (2.2) allows for the definition of the ALE convective velocity $\mathbf{c} = \mathbf{u}^{\mathrm{F}} - \mathbf{u}^{\mathrm{G}}$, representing the fluid velocity relative to the arbitrarily moving fluid domain. The Navier-Stokes equations of the fluid field hence read

$$\frac{\partial \rho^F}{\partial t} + \boldsymbol{\nabla} \cdot (\rho^F \mathbf{c}) = S^c, \tag{2.4}$$

$$\frac{\partial \rho \mathbf{u}^{\mathrm{F}}}{\partial t} + \mathbf{c} \cdot \boldsymbol{\nabla}(\rho \mathbf{u}^{\mathrm{F}}) = \boldsymbol{\nabla} \cdot \boldsymbol{\sigma}^{\mathrm{F}} + \mathbf{S}^m, \tag{2.5}$$

$$\boldsymbol{\sigma}^{\mathrm{F}} = \mu(\boldsymbol{\nabla}\mathbf{u}^{\mathrm{F}} + (\boldsymbol{\nabla}\mathbf{u}^{\mathrm{F}})^T) + \lambda(\boldsymbol{\nabla} \cdot \mathbf{u}^{\mathrm{F}} - p)\mathbf{I}, \tag{2.6}$$

$$\frac{\partial \rho E}{\partial t} + \boldsymbol{\nabla} \cdot (\rho E \mathbf{c}) = \boldsymbol{\nabla} \cdot (\boldsymbol{\sigma}^{\mathrm{F}} \mathbf{u}^{\mathrm{F}}) + \boldsymbol{\nabla} \cdot (\boldsymbol{\kappa}^F \boldsymbol{\nabla} T^F) + S^e, \tag{2.7}$$

and are valid in $\Omega^{\mathrm{F}} \times (0, t_f)$, where fluid density ρ, fluid momentum $\rho \mathbf{u}^{\mathrm{F}}$, and total conservative energy ρE are unknown. To close this set of equations, the present work uses the ideal gas law to calculate the fluid pressure p and temperature T^F. In the second order fluid stress tensor, defined in Eq. (2.6), the bulk viscosity λ is defined as $-\frac{2}{3}\mu$ in the present work, with μ being the fluid viscosity, calculated using the Sutherland model, and $\mathbf{I}$ being the second order identity matrix. The constant $\boldsymbol{\kappa}^F$ is the coefficient of thermal conductivity for the fluid. Finally, S^c, S^m, and S^e, are the source terms for the conservation of mass, momentum, and energy respectively.

Boundary conditions at the Dirichlet boundary $\Gamma_{\mathrm{D}}^{\mathrm{F}}$ and the Neumann boundary $\Gamma_{\mathrm{N}}^{\mathrm{F}}$ can

be stated as

$$\rho^F = \bar{\rho} \quad \text{in} \quad \Gamma^{\mathrm{F}}_{\mathrm{D}} \times (0, t_f), \tag{2.8}$$

$$\mathbf{u}^{\mathrm{F}} = \bar{\mathbf{u}} \quad \text{in} \quad \Gamma^{\mathrm{F}}_{\mathrm{D}} \times (0, t_f), \tag{2.9}$$

$$E = \bar{E} \quad \text{in} \quad \Gamma^{\mathrm{F}}_{\mathrm{D}} \times (0, t_f), \tag{2.10}$$

$$\boldsymbol{\sigma}^{\mathrm{F}} \cdot \hat{\mathbf{n}}^{\mathrm{F}} = \bar{\mathbf{h}}^F \quad \text{in} \quad \Gamma^{\mathrm{F}}_{\mathrm{N}} \times (0, t_f), \tag{2.11}$$

$$\boldsymbol{\kappa}^F \boldsymbol{\nabla} T^F \cdot \hat{\mathbf{n}}^{\mathrm{F}} = \bar{\mathbf{q}}^F \quad \text{in} \quad \Gamma^{\mathrm{F}}_{\mathrm{N}} \times (0, t_f). \tag{2.12}$$

To state the complete initial boundary value problem the unknowns must be given an initial value $\rho^F(\mathbf{x}, 0) = \rho_0^F(\mathbf{x})$, $\rho\mathbf{u}^{\mathrm{F}}(\mathbf{x}, 0) = \rho\mathbf{u}_0^{\mathrm{F}}(\mathbf{x})$, and $\rho E(\mathbf{x}, 0) = \rho E_0(\mathbf{x})$ for $\mathbf{x} \in \Omega^{\mathrm{F}}$.

The weak form of the compressible Navier-Stokes equations (2.4) - (2.7) is obtained by testing these equations with test functions $\delta\rho^F$, $\delta\rho\mathbf{u}^{\mathrm{F}}$, and $\delta\rho E$ for the conservation of mass, momentum, and energy respectively. Then integrating by parts the momentum and energy equations and taking into account that the fluid velocity at an FSI boundary is zero for a no-slip condition results in,

$$0 = \left(\delta\rho^F, \frac{\partial \rho^F}{\partial t} + \boldsymbol{\nabla} \cdot (\rho^F \mathbf{c}) - S^c \right)_{\Omega^{\mathrm{F}}} \tag{2.13}$$

$$\begin{aligned} 0 = &\left(\delta\rho\mathbf{u}^{\mathrm{F}}, \frac{\partial \rho\mathbf{u}^{\mathrm{F}}}{\partial t} + \mathbf{c} \cdot \boldsymbol{\nabla}(\rho\mathbf{u}^{\mathrm{F}}) - S^m \right)_{\Omega^{\mathrm{F}}} + \\ &\left(\boldsymbol{\nabla} \cdot \delta\rho\mathbf{u}^{\mathrm{F}}, \boldsymbol{\sigma}^F \right)_{\Omega^{\mathrm{F}}} - \left(\delta\rho\mathbf{u}^{\mathrm{F}}, \bar{\mathbf{h}}^F \right)_{\Gamma^{\mathrm{F}}_{\mathrm{N}}} + \delta W_{\Gamma}^{Fm} \end{aligned} \tag{2.14}$$

$$\begin{aligned} 0 = &\left(\delta\rho E, \frac{\partial \rho E}{\partial t} + \boldsymbol{\nabla} \cdot (\rho E \mathbf{c}) - S^e \right)_{\Omega^{\mathrm{F}}} + \\ &\left(\boldsymbol{\nabla}\delta\rho E, \boldsymbol{\sigma}^{\mathrm{F}}\mathbf{u}^{\mathrm{F}} + \boldsymbol{\kappa}^F \boldsymbol{\nabla} T^F \right)_{\Omega^{\mathrm{F}}} - \left(\delta\rho E, \bar{\mathbf{q}}^F \right)_{\Gamma^{\mathrm{F}}_{\mathrm{N}}} + \delta W_{\Gamma}^{Fe} \end{aligned} \tag{2.15}$$

where $\delta W_{\Gamma}^{\mathrm{Fm}}$ denotes a contribution of the FSI interface to the momentum equation that will be deduced in Sec. 2.4 and $\delta W_{\Gamma}^{\mathrm{Fe}}$ denotes a contribution of the fluid thermal interface interface to the energy equation that will be deduced in Sec. 2.5. The $(,)_{\Omega^{\mathrm{F}}}$ operator denotes an integral of the product over the domain Ω^{F}.

2.2. *Structure*

In this work we assume a structure field governed by the nonlinear elastodynamics equation

$$\rho^{\mathrm{S}} \frac{\mathrm{d}^2 \mathbf{d}^{\mathrm{S}}}{\mathrm{d}t^2} = \boldsymbol{\nabla} \cdot (\mathbf{F}\mathbf{S}) + \rho^{\mathrm{S}} \mathbf{b}^{\mathrm{S}} \quad \text{in} \quad \Omega^{\mathrm{S}} \times (0, t_f), \tag{2.16}$$

that states an equilibrium between the forces of inertia, internal forces and an external body force $\mathbf{b}^{\mathrm{S}}$ in the undeformed structural configuration Ω^{S}. Given the structural density ρ^{S} defined per unit undeformed volume, Eq. (2.16) has to be solved for the unknown structural displacements $\mathbf{d}^{\mathrm{S}}$. The internal forces are expressed in terms of the second Piola-Kirchhoff stress tensor $\mathbf{S}$ and the deformation gradient $\mathbf{F}$.

Different constitutive relations can be employed in this context, but for the sake of simplicity a hyperelastic material behavior with strain energy function Ψ is considered in the remainder of this paper. The second Piola-Kirchhoff stress tensor $\mathbf{S}$ is thus defined as

$$\mathbf{S} = 2 \frac{\partial \Psi}{\partial \mathbf{C}}, \tag{2.17}$$

where the right Cauchy-Green tensor $\mathbf{C} = \mathbf{F}^{\mathrm{T}}\mathbf{F}$ has been introduced.

The boundary conditions defined on the Dirichlet boundary $\Gamma_{\mathrm{D}}^{\mathrm{S}}$ and on the Neumann boundary $\Gamma_{\mathrm{N}}^{\mathrm{S}}$ read

$$\mathbf{d}^{\mathrm{S}} = \bar{\mathbf{d}}^{\mathrm{S}} \quad \text{in} \quad \Gamma_{\mathrm{D}}^{\mathrm{S}} \times (0, t_f), \tag{2.18}$$

$$(\mathbf{FS}) \cdot \mathbf{N} = \bar{\mathbf{h}}^{\mathrm{S}} \quad \text{in} \quad \Gamma_{\mathrm{N}}^{\mathrm{S}} \times (0, t_f), \tag{2.19}$$

Given initial displacements and velocities $\mathbf{d}_0^{\mathrm{S}}(\mathbf{x})$ and $\dot{\mathbf{d}}_0^{\mathrm{S}}(\mathbf{x})$, respectively, the initial boundary conditions

$$\mathbf{d}^{\mathrm{S}}(\mathbf{x}, 0) = \mathbf{d}_0^{\mathrm{S}}(\mathbf{x}) \quad \text{for} \quad \mathbf{x} \in \Omega^{\mathrm{S}}, \tag{2.20}$$

$$\frac{\mathrm{d}\mathbf{d}^{\mathrm{S}}}{\mathrm{d}t}(\mathbf{x}, 0) = \dot{\mathbf{d}}_0^{\mathrm{S}}(\mathbf{x}) \quad \text{for} \quad \mathbf{x} \in \Omega^{\mathrm{S}}, \tag{2.21}$$

have to be additionally satisfied.

Testing (2.16) with the virtual displacements $\delta\mathbf{d}^{\mathrm{S}}$ and integration by parts yield the weak form

$$\begin{aligned} 0 = &\left(\delta\mathbf{d}^{\mathrm{S}}, \rho^{\mathrm{S}} \frac{\mathrm{d}^2\mathbf{d}^{\mathrm{S}}}{\mathrm{d}t^2}\right)_{\Omega^{\mathrm{S}}} + \left(\boldsymbol{\nabla}\delta\mathbf{d}^{\mathrm{S}}, \mathbf{FS}\right)_{\Omega^{\mathrm{S}}} \\ &- \left(\delta\mathbf{d}^{\mathrm{S}}, \rho^{\mathrm{S}}\mathbf{b}^{\mathrm{S}}\right)_{\Omega^{\mathrm{S}}} - \left(\delta\mathbf{d}^{\mathrm{S}}, \bar{\mathbf{h}}^{\mathrm{S}}\right)_{\Gamma_{\mathrm{N}}^{\mathrm{S}}} + \delta W_{\Gamma}^{\mathrm{Sm}}, \end{aligned} \tag{2.22}$$

which is the starting point for the finite element discretization. The influence of the interface on the structure field is accounted for by $\delta W_{\Gamma}^{\mathrm{Sm}}$, which will be discussed in Sec. 2.4.

2.3. *Thermal*

For this work, it is assumed that the solid material does not change phase and that the specific heat is constant. Based on these assumptions, the thermal field can be described by the following equation,

$$\rho^S C \frac{\partial T^S}{\partial t} + \rho^S C \mathbf{u}^{\mathrm{G}} \cdot \boldsymbol{\nabla} T^S - \boldsymbol{\nabla} \cdot \boldsymbol{\kappa}^S \boldsymbol{\nabla} T^S - S^t = 0 \tag{2.23}$$

where T^S is the unknown temperature field of the structure, C is the specific heat constant, $\boldsymbol{\kappa}^S$ is the thermal conductivity tensor, which can reduce to a single constant for an isotropic material, and S^t is the source term. The term including the mesh velocities, $\mathbf{u}^{\mathrm{G}}$, is an ALE correction for the advection of material due to mesh motion. This is the case in such phenomena as ablation and wear.

Boundary conditions at the Dirichlet boundary $\Gamma_{\mathrm{D}}^{\mathrm{T}}$ and the Neumann boundary $\Gamma_{\mathrm{N}}^{\mathrm{T}}$ can be stated as

$$T^S = \bar{T} \quad \text{in} \quad \Gamma_{\mathrm{D}}^{\mathrm{S}} \times (0, t_f), \tag{2.24}$$

$$\boldsymbol{\kappa}^S \boldsymbol{\nabla} T^S \cdot \hat{\mathbf{n}}^{\mathrm{S}} = \bar{\mathbf{q}} \quad \text{in} \quad \Gamma_{\mathrm{N}}^{\mathrm{S}} \times (0, t_f). \tag{2.25}$$

To state the complete initial boundary value problem the temperature field must be given an initial value $T^S(\mathbf{x}, 0) = T_0^S(\mathbf{x})$ for $\mathbf{x} \in \Omega^{\mathrm{S}}$. The thermal equation can then be made weak by multiplying it with δT^S and integrating by parts, yielding

$$\begin{aligned} 0 = &\left(\delta T^S, \rho^S C \frac{\partial T^S}{\partial t} + \rho^S C \mathbf{u}^{\mathrm{G}} \cdot \boldsymbol{\nabla} T^S - S^t\right)_{\Omega^{\mathrm{S}}} + \\ &\left(\boldsymbol{\nabla}\delta T^S, \boldsymbol{\kappa}^S \boldsymbol{\nabla} T^S\right)_{\Omega^{\mathrm{S}}} - \left(\boldsymbol{\nabla}\delta T^S, \bar{\mathbf{q}}\right)_{\Gamma_N^S} + \delta W_{\Gamma}^{Se}. \end{aligned} \tag{2.26}$$

2.4. *Fluid-Structure Interface*

Coupling of the different fields is realized by enforcing kinematic and dynamic constraints at the fluid-structure interface Γ. Usually, the no-slip boundary condition

$$\frac{\partial \mathbf{d}_\Gamma^{\mathrm{S}}}{\partial t} = \mathbf{u}_\Gamma^{\mathrm{F}} \quad \text{in} \quad \Gamma \times (0, t_f) \tag{2.27}$$

is applied, which prohibits both a mass flow across and a relative tangential movement of fluid and structure at the fluid-structure interface. In combination with (2.3) this condition (2.27) is equivalent to

$$\mathbf{d}_\Gamma^{\mathrm{S}} = \mathbf{d}_\Gamma^{\mathrm{G}} \quad \text{in} \quad \Gamma \times (0, t_f) \tag{2.28}$$

stating that structural deformation and fluid movement (represented by the ALE based fluid domain deformation $\mathbf{d}_\Gamma^{\mathrm{G}}$) must match on Γ. In addition, equilibrium of forces requires the surface tractions of fluid and structure to be equal, yielding

$$\mathbf{h}_\Gamma^{\mathrm{S}} = -\mathbf{h}_\Gamma^{\mathrm{F}} \quad \text{in} \quad \Gamma \times (0, t_f), \tag{2.29}$$

where $\mathbf{h}$ is the unknown surface traction at the interface.

In preparation of the mortar finite element discretization to follow, the method of weighted residuals is applied to the interface conditions. By introducing the Lagrange multiplier field $\boldsymbol{\lambda}$ and corresponding test functions $\delta\boldsymbol{\lambda}$ on the fluid-structure interface Γ, we obtain the weak form

$$\left(\delta\boldsymbol{\lambda}, \mathbf{d}_\Gamma^{\mathrm{S}} - \mathbf{d}_\Gamma^{\mathrm{G}}\right)_\Gamma = 0. \tag{2.30}$$

This adds an integral version of the continuity constraint (2.28) to the general problem definition. Furthermore, the unknown surface tractions introduced in (2.29) have to be imposed in a weak sense on the respective physical field, yielding the missing coupling terms in fluid weak form (2.14) and structure weak form (2.22)

$$\delta W_\Gamma^{\mathrm{Fm}} = \left(\mathbf{h}_\Gamma^{\mathrm{F}}, \delta\rho\mathbf{u}_\Gamma^{\mathrm{F}}\right)_\Gamma, \tag{2.31}$$

$$\delta W_\Gamma^{\mathrm{Sm}} = \left(\mathbf{h}_\Gamma^{\mathrm{S}}, \delta\mathbf{d}_\Gamma^{\mathrm{S}}\right)_\Gamma. \tag{2.32}$$

Identifying the Lagrange multiplier field $\boldsymbol{\lambda}$ with the unknown surface traction $\mathbf{h}_\Gamma^{\mathrm{S}} = -\mathbf{h}_\Gamma^{\mathrm{F}}$, these coupling terms can be expressed as

$$\delta W_\Gamma^{\mathrm{Fm}} = -\left(\boldsymbol{\lambda}, \delta\rho\mathbf{u}_\Gamma^{\mathrm{F}}\right)_\Gamma, \tag{2.33}$$

$$\delta W_\Gamma^{\mathrm{Sm}} = \quad \left(\boldsymbol{\lambda}, \delta\mathbf{d}_\Gamma^{\mathrm{S}}\right)_\Gamma. \tag{2.34}$$

Thus, fluid-structure coupling is established in a weak sense, which formally leads to a four field FSI system, not considering the thermal field.

2.5. *Fluid-Thermal Interface*

The fluid thermal interface requires that there not be a jump in temperature and heat fluxes across the boundary must be satisfied as shown in the following equations,

$$T_\Gamma^{\mathrm{S}} = T_\Gamma^{\mathrm{F}} \quad \text{in} \quad \Gamma \times (0, t_f), \tag{2.35}$$

$$\boldsymbol{\kappa}^S \boldsymbol{\nabla} T^S \cdot \hat{\mathbf{n}}^{\mathrm{S}} = -\boldsymbol{\kappa}^F \boldsymbol{\nabla} T^F \cdot \hat{\mathbf{n}}^{\mathrm{F}} \quad \text{in} \quad \Gamma \times (0, t_f). \tag{2.36}$$

In the case where there is material advection due to non-linear surface effects, an ALE formulation is used for the thermal field and Eqs. (2.27) and (2.28) must be modified to include the mesh displacements due to these effects. The work during this research

project has not yet addressed the fluid thermal interactions, particularly for the case of a thermal ALE formulation. This is however part of the planned future work.

The remainder of this report will focus on the dual mortar method. The presentation of the dual mortar method will be in the context of incompressible fluid structure interaction however. This is because in the incompressible Navier-Stokes equations velocities are the unknowns as apposed the momentum unknowns in the conservative form of the compressible Navier-Stokes equations. This is much simpler as the relationship between the fluid velocities and the mesh displacements is linear, where as the relationship in the compressible versions is dependent on multiple unknowns and therefore the condensation of the system is non-trivial.

3. Finite element discretization and mortar coupling

The field equations are discretized in space and time, but the actual discretization is of little importance for the monolithic approach presented here. In general, we use implicit time integration schemes and finite elements for fluid, ALE and structure fields, leading to a set of nonlinear algebraic equations. The interface conditions are enforced using a dual mortar method, augmenting the system of equations with a fourth field. The complete nonlinear FSI problem is solved using a Newton-type method, where a set of corresponding linearized equations has to be solved in every iteration step of the algorithm.

Note that the equivalence of (2.27) and (2.28) only holds in the continuous setting. In the discrete setting, one of these two equations may not be satisfied exactly, if different time integration schemes are used for the different fields. This effect, which is well-known in fluid-structure interaction, can usually be considered negligible. Since it is also neither connected to monolithic coupling schemes nor to the mortar approach proposed here, a detailed investigation is not carried out in the present contribution.

In the following the resulting sets of linearized equations for fluid and structure are briefly introduced. The derivation of the interface equations is shown in more detail. Finally, the complete linearized FSI system is stated.

3.1. *Fluid*

In the applications shown here, stabilized finite elements are used to discretize the fluid. Stabilization terms are applied to account for instabilities arising from equal-order discretization of fluid and pressure fields as well as for convection-dominated problems. For details on the finite element discretization of the fluid field and stabilization methods we refer e.g. to [13], to the monograph [14] or to the review article [15].

For time discretization a one-step-θ scheme or a BDF2 scheme are used. Both integration schemes assume a constant acceleration within a time step, although they approximate its value differently. This implies a second order discretization of the interface velocity yielding

$$\mathbf{d}_\Gamma^{\mathrm{G},n+1} = \mathbf{d}_\Gamma^{\mathrm{G},n} + \frac{\Delta t}{2}\left(\mathbf{u}_\Gamma^{\mathrm{F},n+1} + \mathbf{u}_\Gamma^{\mathrm{F},n}\right), \tag{3.1}$$

where we have used the fact, that grid and fluid velocities match at the interface according to (2.3). In (3.1), $\mathbf{d}^{\mathrm{G},n}$ and $\mathbf{u}^{\mathrm{F},n}$ denote the vector of *discrete* nodal displacements and velocities, respectively, in time step n. In the following the time step index may be omitted to shorten the notation if not necessary for understanding.

The Newton-type method used to solve the monolithic FSI system requires a consistent linearization of the fluid residual $\mathbf{f}^{\mathrm{F}} = \mathbf{f}^{\mathrm{F}}(\mathbf{u}^{\mathrm{F}}, \mathbf{p}^{\mathrm{F}}, \mathbf{d}^{\mathrm{G}})$ that represents the discretized right hand side of the weak form of the conservation of momentum for an incompressible fluid. The total residual differential becomes

$$\mathrm{d}\mathbf{f}^{\mathrm{F}} = \frac{\partial \mathbf{f}^{\mathrm{F}}}{\partial \mathbf{u}^{\mathrm{F}}} \mathrm{d}\mathbf{u}^{\mathrm{F}} + \frac{\partial \mathbf{f}^{\mathrm{F}}}{\partial \mathbf{p}^{\mathrm{F}}} \mathrm{d}\mathbf{p}^{\mathrm{F}} + \frac{\partial \mathbf{f}^{\mathrm{F}}}{\partial \mathbf{d}^{\mathrm{G}}} \mathrm{d}\mathbf{d}^{\mathrm{G}}. \tag{3.2}$$

In the following the vector $\mathbf{p}^{\mathrm{F}}$ of nodal pressure values is dropped from the notation and merged in the fluid's interior unknowns $\mathbf{u}^{\mathrm{F}}_{\mathrm{I}}$. The split into quantities defined in the interior of the domain (denoted by $\cdot_{\mathrm{I}}$) and those defined on the interface (denoted by $\cdot_{\Gamma}$) yields the following matrix representation of the partial derivatives introduced in (3.2):

$$\mathbf{F}_{\alpha\beta} = \frac{\partial \mathbf{f}^{\mathrm{F}}_{\alpha}}{\partial \mathbf{u}^{\mathrm{F}}_{\beta}}, \quad \mathbf{F}^{\mathrm{G}}_{\alpha\beta} = \frac{\partial \mathbf{f}^{\mathrm{F}}_{\alpha}}{\partial \mathbf{d}^{\mathrm{G}}_{\beta}}, \tag{3.3}$$

with $\alpha, \beta \in \{\mathrm{I}, \Gamma\}$. For a detailed description of the fluid shape derivatives $\mathbf{F}^{\mathrm{G}}_{\alpha\beta}$ the reader is referred to [16, 17].

The Jacobian system for the Newton method can be formulated as

$$\frac{\mathrm{d}\mathbf{f}^{\mathrm{F}}}{\mathrm{d}\mathbf{x}^{\mathrm{F}}} \boldsymbol{\Delta}\mathbf{x}^{\mathrm{F}}_{i} = -\mathbf{f}^{\mathrm{F}}_{i} \tag{3.4}$$

where $i \geq 0$ denotes the iteration step and $\mathbf{x}^{\mathrm{F}}$ the vector of unknowns of the fluid problem including mesh deformations. In detail the fluid system of equations for time step $n+1$ reads

$$\begin{aligned} \begin{bmatrix} \mathbf{F}_{\mathrm{II}} & \mathbf{F}_{\mathrm{I}\Gamma} & \mathbf{F}^{\mathrm{G}}_{\mathrm{II}} & \mathbf{F}^{\mathrm{G}}_{\mathrm{I}\Gamma} \\ \mathbf{F}_{\Gamma\mathrm{I}} & \mathbf{F}_{\Gamma\Gamma} & \mathbf{F}^{\mathrm{G}}_{\Gamma\mathrm{I}} & \mathbf{F}^{\mathrm{G}}_{\Gamma\Gamma} \end{bmatrix} \begin{bmatrix} \boldsymbol{\Delta}\mathbf{u}^{\mathrm{F},n+1}_{\mathrm{I},i} \\ \boldsymbol{\Delta}\mathbf{u}^{\mathrm{F},n+1}_{\Gamma,i} \\ \boldsymbol{\Delta}\mathbf{d}^{\mathrm{G},n+1}_{\mathrm{I},i} \\ \boldsymbol{\Delta}\mathbf{d}^{\mathrm{G},n+1}_{\Gamma,i} \end{bmatrix} = \\ - \begin{bmatrix} \mathbf{f}^{\mathrm{F},n+1}_{\mathrm{I},i} \\ \mathbf{f}^{\mathrm{F},n+1}_{\Gamma,i} \end{bmatrix} - \begin{bmatrix} \mathbf{0} \\ \mathbf{f}^{\mathrm{F},n+1}_{\boldsymbol{\lambda},i} \end{bmatrix}, \end{aligned} \tag{3.5}$$

where $\mathbf{f}^{\mathrm{F},n+1}_{\boldsymbol{\lambda},i}$ accounts for the contributions of the unknown discrete Lagrange multiplier on the traction at the interface and corresponds to (2.33).

The mesh movement is governed by (2.1) and we assume that discretization and linearization result in an ALE system matrix $\mathbf{A}$. Since the mesh movement is not allowed to influence the physical solution at the interface, the set of linear equations reduces to

$$\begin{bmatrix} \mathbf{A}_{\mathrm{II}} & \mathbf{A}_{\mathrm{I}\Gamma} \end{bmatrix} \begin{bmatrix} \boldsymbol{\Delta}\mathbf{d}^{\mathrm{G}}_{\mathrm{I}i} \\ \boldsymbol{\Delta}\mathbf{d}^{\mathrm{G}}_{\Gamma,i} \end{bmatrix} = \mathbf{0}. \tag{3.6}$$

The mesh interface displacement increments $\boldsymbol{\Delta}\mathbf{d}^{\mathrm{G}}_{\Gamma}$ can now be substituted in terms of the fluid interface velocity employing (3.1):

$$\boldsymbol{\Delta}\mathbf{d}^{\mathrm{G},n+1}_{\Gamma,i} = \begin{cases} \frac{\Delta t}{2} \boldsymbol{\Delta}\mathbf{u}^{\mathrm{F},n+1}_{\Gamma,i} + \Delta t\, \mathbf{u}^{\mathrm{F},n}_{\Gamma} & \text{for} \quad i = 0 \\ \frac{\Delta t}{2} \boldsymbol{\Delta}\mathbf{u}^{\mathrm{F},n+1}_{\Gamma,i} & \text{for} \quad i > 0 \end{cases}. \tag{3.7}$$

Applying (3.7) to (3.5) and (3.6) yields the final system of equations for fluid and ALE

field

$$\begin{bmatrix} \mathbf{F}_{\mathrm{II}} & \mathbf{F}_{\mathrm{I}\Gamma} + \frac{\Delta t}{2}\mathbf{F}^{\mathrm{G}}_{\mathrm{II}} & \mathbf{F}^{\mathrm{G}}_{\mathrm{II}} \\ \mathbf{F}_{\Gamma\mathrm{I}} & \mathbf{F}_{\Gamma\Gamma} + \frac{\Delta t}{2}\mathbf{F}^{\mathrm{G}}_{\Gamma\Gamma} & \mathbf{F}^{\mathrm{G}}_{\Gamma\mathrm{I}} \\ \mathbf{0} & \frac{\Delta t}{2}\mathbf{A}_{\mathrm{I}\Gamma} & \mathbf{A}_{\mathrm{II}} \end{bmatrix} \begin{bmatrix} \boldsymbol{\Delta}\mathbf{u}^{\mathrm{F},n+1}_{\mathrm{I},i} \\ \boldsymbol{\Delta}\mathbf{u}^{\mathrm{F},n+1}_{\Gamma,i} \\ \boldsymbol{\Delta}\mathbf{d}^{\mathrm{F},n+1}_{\mathrm{I},i} \end{bmatrix} = -\tilde{\mathbf{f}}^{\mathrm{F},n+1}_{i}. \tag{3.8}$$

The modified fluid residual vector $\tilde{\mathbf{f}}^{\mathrm{F},n+1}_{i}$ depends on the iteration step i:

$$\tilde{\mathbf{f}}^{\mathrm{F},n+1}_{i} = \begin{bmatrix} \mathbf{f}^{\mathrm{F},n+1}_{\mathrm{I},i} \\ \mathbf{f}^{\mathrm{F},n+1}_{\Gamma,i} + \mathbf{f}^{\mathrm{F},n+1}_{\boldsymbol{\lambda},i} \\ \mathbf{0} \end{bmatrix} + \chi(i)\Delta t \begin{bmatrix} \mathbf{F}^{\mathrm{G}}_{\mathrm{I}\Gamma}\mathbf{u}^{\mathrm{F},n}_{\Gamma} \\ \mathbf{F}^{\mathrm{G}}_{\Gamma\Gamma}\mathbf{u}^{\mathrm{F},n}_{\Gamma} \\ \mathbf{A}_{\mathrm{I}\Gamma}\mathbf{u}^{\mathrm{F},n}_{\Gamma} \end{bmatrix}, \tag{3.9}$$

where we have introduced the mapping

$$\chi(i) = \begin{cases} 1, & i = 0 \\ 0, & i > 0 \end{cases} \tag{3.10}$$

to shorten the notation.

3.2. *Structure*

As it is true for the fluid discretization, the algorithms discussed here are not restricted to any specific discretization of the structure equations. We consider a discretization with mixed/hybrid finite elements. Several countermeasures against various locking phenomena are implemented, e.g. enhanced assumed strains (EAS), assumed natural strains (ANS) or mixed formulations with additional degrees of freedom for a structural pressure. Details about the finite element method for structure fields can be found in [18, 19].

The generalized-α time integration scheme proposed in [20] has shown to be an efficient and robust method for dynamic structure simulations. This scheme offers second-order accuracy in combination with the possibility of numerical damping and is used in the applications discussed in this work.

To derive the structure contributions to the FSI system we start with the right hand side of the discretized weak form (2.22) denoted by the residual $\mathbf{f}^{\mathrm{S}} = \mathbf{f}^{\mathrm{S}}(\mathbf{d}^{\mathrm{S}})$, where $\mathbf{d}^{\mathrm{S}}$ is from now on the vector of *discretized* nodal displacements. The structure stiffness matrix $\mathbf{S}$ is again split into interior quantities $(\cdot_{\mathrm{I}})$ and those defined on the interface Γ

$$\mathbf{S}_{\alpha\beta} = \frac{\partial \mathbf{f}^{\mathrm{S}}_{\alpha}}{\partial \mathbf{d}^{\mathrm{S}}_{\beta}}, \tag{3.11}$$

given $\alpha, \beta \in \{\mathrm{I}, \Gamma\}$. The complete linear system to be solved in every iteration step i of the non-linear algorithm then reads

$$\begin{bmatrix} \mathbf{S}_{\mathrm{II}} & \mathbf{S}_{\mathrm{I}\Gamma} \\ \mathbf{S}_{\Gamma\mathrm{I}} & \mathbf{S}_{\Gamma\Gamma} \end{bmatrix} \begin{bmatrix} \boldsymbol{\Delta}\mathbf{d}^{\mathrm{S},n+1}_{\mathrm{I},i} \\ \boldsymbol{\Delta}\mathbf{d}^{\mathrm{S},n+1}_{\Gamma,i} \end{bmatrix} = - \begin{bmatrix} \mathbf{f}^{\mathrm{S},n+1}_{\mathrm{I},i} \\ \mathbf{f}^{\mathrm{S},n+1}_{\Gamma,i} \end{bmatrix} - \begin{bmatrix} \mathbf{0} \\ \mathbf{f}^{\mathrm{S},n+1}_{\boldsymbol{\lambda},i} \end{bmatrix} \tag{3.12}$$

for time step $n+1$. The contribution of the unknown Lagrange multiplier at the FSI interface corresponding to (2.34) is denoted by $\mathbf{f}^{\mathrm{S},n+1}_{\boldsymbol{\lambda},i}$.

3.3. *Fluid-structure interface*

Non-conforming finite element discretization brings about that fluid and structure surfaces at the FSI interface Γ do not match any more, as it has been the case in the continuous setting and when using node-matching interface meshes. In the context of the mortar method, this makes the choice of so-called *slave* and *master* sides Γ^{sl} and

Γ^{ma} necessary. The Lagrange multiplier field is then discretized on the slave side of the interface and numerical integration of the coupling terms is also performed there.

3.3.1. *The dual mortar method*

For making the following derivations more general, we introduce the displacement fields $\mathbf{d}_{\Gamma}^{\mathrm{sl}}$ and $\mathbf{d}_{\Gamma}^{\mathrm{ma}}$ and derive the dual mortar method as an abstract coupling strategy for two non-conforming meshes. Of course, a concrete choice of fluid or structure field being the slave side has to be made when using this approach within the proposed FSI framework. This choice and its effect on the monolithic FSI schemes presented here will be investigated in Sec. 4. The general form of slave and master displacement interpolation reads

$$\mathbf{d}_{\Gamma}^{\mathrm{sl}} = \sum_{k=1}^{n^{\mathrm{sl}}} N_k^{\mathrm{sl}} \mathbf{d}_k^{\mathrm{sl}} \,, \quad \mathbf{d}_{\Gamma}^{\mathrm{ma}} = \sum_{l=1}^{n^{\mathrm{ma}}} N_l^{\mathrm{ma}} \mathbf{d}_l^{\mathrm{ma}} \,, \tag{3.13}$$

where shape functions N_k^{sl}, N_l^{ma} are obtained based on their trace space relationship with the underlying discretizations of the domains 'behind' the mortar interface (in this context fluid and structure domains). Nodal displacements are represented by $\mathbf{d}_k^{\mathrm{sl}}$, $\mathbf{d}_l^{\mathrm{ma}}$. The total number of slave and master nodes is given by n^{sl} and n^{ma}, respectively.

Within the *dual* mortar method considered here, the Lagrange multiplier interpolation on the slave side of the interface is based on so-called dual shape functions Φ_j as

$$\boldsymbol{\lambda} = \sum_{j=1}^{n^{\mathrm{sl}}} \Phi_j \boldsymbol{\lambda}_j \,, \tag{3.14}$$

with discrete nodal Lagrange multipliers $\boldsymbol{\lambda}_j$. The dual shape functions are constructed such that a biorthogonality condition, as introduced in [10, 11, 21], is satisfied, yielding

$$\int_{\Gamma^{\mathrm{sl}}} \Phi_j N_k^{\mathrm{sl}} \mathrm{d}\Gamma = \delta_{jk} \int_{\Gamma^{\mathrm{sl}}} N_k^{\mathrm{sl}} \mathrm{d}\Gamma, \tag{3.15}$$

where δ_{jk} is the Kronecker delta. Note that (3.15) demands an evaluation of shape function integrals on the actual (possibly distorted) surface element geometry in the reference configuration. Therefore, an *a priori* definition of dual shape functions is not possible in general, but these ansatz functions for Lagrange multiplier interpolation become element-specific. Figure 1 exemplarily shows (standard) displacement shape functions and (dual) Lagrange multiplier shape functions for a 3-node triangular and for an undistorted 4-node quadrilateral surface element. For a more detailed overview and exemplary local calculations of element-specific dual shape functions for 3D mortar coupling, we refer to [4, 8, 22].

Furthermore, a modification of the Lagrange multiplier interpolation at so-called cross-points, where more than two subdomains with non-matching grids meet, becomes necessary. The same is true for interface edges where Dirichlet boundary conditions are prescribed. In simple terms, this modification is based on removing the discrete Lagrange multipliers from the affected points or edges to avoid over-constraint. However, the constant value interpolation property must be retained throughout this process, as visualized for the 2D dual mortar case in Fig. 2. Further details of such modifications can be found in [9, 11].

For the sake of clarity, we temporarily ignore the weak continuity condition (2.30)

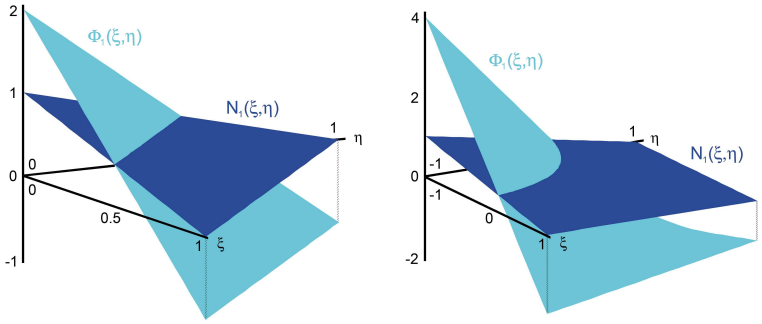

(a) 3-node triangular surface elements

(b) undistorted 4-node quadrilateral surface elements

FIGURE 1. Exemplary shape functions $N_1(\xi, \eta)$ and dual shape functions $\Phi_1(\xi, \eta)$.

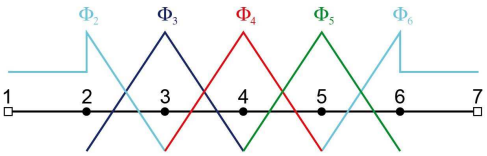

FIGURE 2. Dual shape functions Φ_j for 2D mortar coupling with modifications to allow for cross–points or Dirichlet boundary conditions. The two end nodes 1 and 7 do *not* carry discrete Lagrange multipliers in this case.

already derived for the concrete FSI setting and instead consider the more general form

$$\left(\delta\boldsymbol{\lambda}, \mathbf{d}_\Gamma^{\mathrm{sl}} - \mathbf{d}_\Gamma^{\mathrm{ma}}\right)_\Gamma = 0 \tag{3.16}$$

in the following, which couples slave and master displacements of an abstract non-conforming interface. When the interpolations (3.13) and (3.14) are substituted into (3.16), the nodal blocks of two mortar integral matrices $\mathbf{D}$ and $\mathbf{M}$ emerge as

$$\mathbf{D}\,[j,k] = \mathrm{D}_{jk}\mathbf{I}_3 = \int_{\Gamma^{\mathrm{sl}}} \Phi_j N_k^{\mathrm{sl}} \mathrm{d}\Gamma\ \mathbf{I}_3\,, \tag{3.17}$$

$$\mathbf{M}\,[j,l] = \mathrm{M}_{jl}\mathbf{I}_3 = \int_{\Gamma^{\mathrm{sl}}} \Phi_j N_l^{\mathrm{ma}} \mathrm{d}\Gamma\ \mathbf{I}_3\,, \tag{3.18}$$

with the 3×3 identity matrix $\mathbf{I}_3$. Herein, $\mathbf{D}$ is a square $3n^{\mathrm{sl}} \times 3n^{\mathrm{sl}}$ matrix, whereas the definition of $\mathbf{M}$ generally yields a rectangular matrix of dimensions $3n^{\mathrm{sl}} \times 3n^{\mathrm{ma}}$. Inserting the biorthogonality relation (3.15) into (3.17) allows for the advantageous simplification of $\mathbf{D}$ to become a diagonal matrix with nodal blocks

$$\mathbf{D}\,[j,k] = \mathrm{D}_{jk}\mathbf{I}_3 = \delta_{jk} \int_{\Gamma^{\mathrm{sl}}} N_k^{\mathrm{sl}} \mathrm{d}\Gamma\ \mathbf{I}_3\,. \tag{3.19}$$

Finally, the discrete form of the general weak continuity condition (3.16) reads

$$\mathbf{D}\mathbf{d}_\Gamma^{\mathrm{sl}} - \mathbf{M}\mathbf{d}_\Gamma^{\mathrm{ma}} = \mathbf{0}, \tag{3.20}$$

which naturally defines a discrete projection from master displacements to slave displacements as

$$\mathbf{d}_\Gamma^{\mathrm{sl}} = \mathbf{D}^{-1}\mathbf{M}\mathbf{d}_\Gamma^{\mathrm{ma}}. \tag{3.21}$$

Equation (3.21) illustrates one major advantage of the dual mortar approach as compared with standard mortar schemes. The discrete projection operator

$$\mathbf{P} = \mathbf{D}^{-1}\mathbf{M} \tag{3.22}$$

at a non-conforming interface can be applied locally based on the trivial inversion of the diagonal matrix $\mathbf{D}$. Thus, evaluating (3.21) does not require the solution of a possibly large linear system of equations. This evades the high computational cost associated with standard mortar coupling of two non-conforming grids and thus resolves the concerns sometimes raised in this context [23].

For the sake of completeness, it is pointed out that also matching grids are contained in the proposed mortar formulation as a special case, yielding the identity projection operator $\mathbf{P} = \mathbf{I}$.

3.3.2. *Notation for fluid-structure coupling*

We return to the actual fluid-structure interface conditions defined in Sec. 2.4. The discrete form of the weak continuity condition (2.30) is represented by $\mathbf{g} = \mathbf{g}(\mathbf{d}_\Gamma^{\mathrm{S}}, \mathbf{d}_\Gamma^{\mathrm{G}})$, where $\mathbf{d}_\Gamma^{\mathrm{S}}$ and $\mathbf{d}_\Gamma^{\mathrm{G}}$ are the vectors of *discretized* nodal structure and ALE displacements at the interface Γ. Thus, the coupling equation to be solved in every solution step i of the non-linear algorithm reads

$$\left[\begin{array}{cc} \mathbf{C}_{\mathrm{S}} & -\mathbf{C}_{\mathrm{F}} \end{array} \right] \left[\begin{array}{c} \boldsymbol{\Delta}\mathbf{d}_{\Gamma,i}^{\mathrm{S},n+1} \\ \boldsymbol{\Delta}\mathbf{d}_{\Gamma,i}^{\mathrm{G},n+1} \end{array} \right] = \mathbf{0}, \tag{3.23}$$

where $\mathbf{C}_{\mathrm{S}}$ and $\mathbf{C}_{\mathrm{F}}$ are discrete structure and fluid coupling matrices:

$$\mathbf{C}_{\mathrm{S}} = \frac{\partial \mathbf{g}}{\partial \mathbf{d}_\Gamma^{\mathrm{S}}}, \quad \mathbf{C}_{\mathrm{F}} = \frac{\partial \mathbf{g}}{\partial \mathbf{d}_\Gamma^{\mathrm{G}}}. \tag{3.24}$$

In the final linear system of equations (3.8) and (3.9) for fluid and ALE fields the coupling term can be identified as

$$\mathbf{f}_{\boldsymbol{\lambda},i}^{\mathrm{F},n+1} = -\mathbf{C}_{\mathrm{F}}^{\mathrm{T}} \boldsymbol{\lambda}_i^{n+1} \tag{3.25}$$

which is a discrete version of (2.33). Note that $\boldsymbol{\lambda}_i^{n+1}$ now represents the vector of *discretized* nodal Lagrange multipliers at nonlinear solution step i of timestep $n+1$. Similarly, the final system of equations (3.12) for the structure field is completed by the coupling term

$$\mathbf{f}_{\boldsymbol{\lambda},i}^{\mathrm{S},n+1} = \mathbf{C}_{\mathrm{S}}^{\mathrm{T}} \boldsymbol{\lambda}_i^{n+1} \tag{3.26}$$

which is a discrete version of (2.34).

Depending on the choice of structure or fluid as slave side for the mortar approach described above, the discrete coupling matrices $\mathbf{C}_{\mathrm{F}}$ and $\mathbf{C}_{\mathrm{S}}$ can be identified with the mortar matrices $\mathbf{D}$ and $\mathbf{M}$. A global saddle point type monolithic system of equations including fluid and structure discretization as well as the coupling terms derived above will be presented in Sec. 3.4.

3.3.3. *Evaluation of mortar integrals*

As the main focus of the present contribution is on the application of the dual mortar method to non-conforming monolithic FSI simulations, the actual numerical integration of coupling terms is not discussed in detail, but will only be outlined schematically. Figure 3 gives an overview of the main steps associated with the evaluation of the discrete

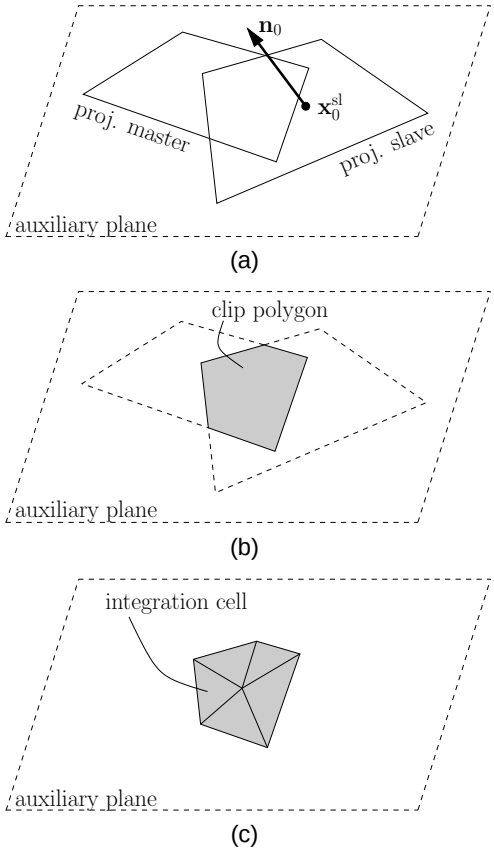

FIGURE 3. Main steps of 3D mortar coupling for one slave and master element pair: (a) construct an auxiliary plane from slave element center $\mathbf{x}_0^{\mathrm{sl}}$ and center normal $\mathbf{n}_0$ and project slave and master nodes onto this plane, (b) perform polygon clipping, (c) divide clip polygon into triangular integration cells and perform Gaussian integration.

mortar integral terms (3.18) and (3.19) in 3D. Obviously, suitable mortar segments for consistent numerical integration need to be constructed. The mortar segments are defined in such a way that the shape functions integrands in (3.18) are continuous on these interface subsets. In 3D situations, this yields arbitrarily shaped polygons as can be seen from Fig. 3(b).

To assure exact conservation of linear momentum, the slave side contributions in (3.19) are integrated using the above defined mortar segments, too [4]. Moreover, exact conservation of angular momentum and thus rotational invariance of the mortar constraints is achieved by applying a simple mesh initialization strategy based on nodal relocation as proposed in [9].

The additional computational cost as compared with a conforming situation is virtually negligible for the pure mesh tying case considered here. It is sufficient to evaluate $\mathbf{D}$ and $\mathbf{M}$ once during initialization. Thereafter, the discrete coupling terms remain unchanged, even though the coupled domains may exhibit finite deformations.

For further details on the numerical integration algorithms in both 2D and 3D the interested reader is referred to the original work by Puso *et al.* [5,6,9] and to the authors' recent work on dual mortar methods for contact analysis [3,4].

3.4. *Monolithic FSI system*

In this paragraph we briefly derive the fully coupled monolithic linear system of equations, where all four discretized and linearized fields are considered: fluid, ALE, structure and the interface Lagrange multipliers.

We start by reformulating the weak coupling condition (3.23). The coupling condition is formulated in terms of the increments $\boldsymbol{\Delta}\mathbf{d}_{\Gamma,i}^{\mathrm{G},n+1}$ at the FSI interface, which have already been eliminated from the fluid system (3.8) in Sec. 3.1. Applying Eq. (3.7) to (3.23) generates the modified coupling condition

$$\begin{bmatrix} \mathbf{C}_{\mathrm{S}} & -\frac{\Delta t}{2}\mathbf{C}_{\mathrm{F}} \end{bmatrix} \begin{bmatrix} \boldsymbol{\Delta}\mathbf{d}_{\Gamma,i}^{\mathrm{S},n+1} \\ \boldsymbol{\Delta}\mathbf{u}_{\Gamma,i}^{\mathrm{F},n+1} \end{bmatrix} = \chi(i)\Delta t \mathbf{C}_{\mathrm{F}}\mathbf{u}_{\Gamma}^{\mathrm{F},n}, \tag{3.27}$$

with $\chi(i)$ defined in (3.10).

With (3.8), (3.12), (3.25), (3.26) and (3.27) we have all necessary relations at hand to state the complete Jacobian monolithic system in timestep $n+1$:

$$\mathbf{J}\boldsymbol{\Delta}\mathbf{x}_i^{n+1} = -\mathbf{f}_i^{n+1}, \tag{3.28}$$

where i denotes the iteration step of the Newton-like method. The FSI residual $\mathbf{f}_i^{n+1}$ is defined as

$$\mathbf{f}_i^{n+1} = \begin{bmatrix} \mathbf{f}_{\mathrm{I},i}^{\mathrm{S},n+1} \\ \mathbf{f}_{\Gamma,i}^{\mathrm{S},n+1} \\ \mathbf{f}_{\mathrm{I},i}^{\mathrm{F},n+1} \\ \mathbf{f}_{\Gamma,i}^{\mathrm{F},n+1} \\ \mathbf{0} \\ \mathbf{0} \end{bmatrix} + \chi(i)\Delta t \begin{bmatrix} \mathbf{0} \\ \mathbf{0} \\ \mathbf{F}_{\mathrm{I}\Gamma}^{\mathrm{G}}\mathbf{u}_{\Gamma}^{\mathrm{F},n} \\ \mathbf{F}_{\Gamma\Gamma}^{\mathrm{G}}\mathbf{u}_{\Gamma}^{\mathrm{F},n} \\ \mathbf{A}_{\mathrm{I}\Gamma}\mathbf{u}_{\Gamma}^{\mathrm{F},n} \\ \mathbf{C}_{\mathrm{F}}\mathbf{u}_{\Gamma}^{\mathrm{F},n} \end{bmatrix}. \tag{3.29}$$

The vector $\mathbf{x}$ contains all unknowns from the four fields of the coupled problem and its increment $\boldsymbol{\Delta}\mathbf{x}_i^{n+1}$ reads

$$\boldsymbol{\Delta}\mathbf{x}_i^{n+1} = \begin{bmatrix} \boldsymbol{\Delta}\mathbf{d}_{\mathrm{I},i}^{\mathrm{S},n+1} \\ \boldsymbol{\Delta}\mathbf{d}_{\Gamma,i}^{\mathrm{S},n+1} \\ \boldsymbol{\Delta}\mathbf{u}_{\mathrm{I},i}^{\mathrm{F},n+1} \\ \boldsymbol{\Delta}\mathbf{u}_{\Gamma,i}^{\mathrm{F},n+1} \\ \boldsymbol{\Delta}\mathbf{d}_{\mathrm{I},i}^{\mathrm{G},n+1} \\ \boldsymbol{\lambda}_i^{n+1} \end{bmatrix}. \tag{3.30}$$

Finally the Jacobian matrix $\mathbf{J} = \frac{\mathrm{d}\mathbf{f}_i^{n+1}}{\mathrm{d}\mathbf{x}_i^{n+1}}$ is:

$$\mathbf{J} = \begin{bmatrix} \mathbf{S}_{\mathrm{II}} & \mathbf{S}_{\mathrm{I}\Gamma} & & & & \\ \mathbf{S}_{\Gamma\mathrm{I}} & \mathbf{S}_{\Gamma\Gamma} & & & & \mathbf{C}_{\mathrm{S}}^{\mathrm{T}} \\ & & \mathbf{F}_{\mathrm{II}} & \mathbf{F}_{\mathrm{I}\Gamma} + \frac{\Delta t}{2}\mathbf{F}_{\mathrm{I}\Gamma}^{\mathrm{G}} & \mathbf{F}_{\mathrm{II}}^{\mathrm{G}} & \\ & & \mathbf{F}_{\Gamma\mathrm{I}} & \mathbf{F}_{\Gamma\Gamma} + \frac{\Delta t}{2}\mathbf{F}_{\Gamma\Gamma}^{\mathrm{G}} & \mathbf{F}_{\Gamma\mathrm{I}}^{\mathrm{G}} & -\mathbf{C}_{\mathrm{F}}^{\mathrm{T}} \\ & & \mathbf{0} & \frac{\Delta t}{2}\mathbf{A}_{\mathrm{I}\Gamma} & \mathbf{A}_{\mathrm{II}} & \\ & \mathbf{C}_{\mathrm{S}} & & -\frac{\Delta t}{2}\mathbf{C}_{\mathrm{F}} & & \end{bmatrix}. \tag{3.31}$$

In general, the linear system (3.28) is hard to solve with iterative linear solvers given the saddle point type structure of (3.31). Therefore, the Lagrange multipliers will be condensed and the problem reduced to a three field problem containing only structure, fluid

and ALE degrees of freedom. In the following section it will be shown that, independent of the particular choice of slave and master discretization, the resulting systems of equations are similar to the system obtained with conforming meshes [1] and hence allow for an efficient use of iterative solution schemes.

4. Condensed systems and iterative solvers

In this section two variants are presented to reduce the saddle point type system (3.31). In both cases the field of Lagrange multiplier is removed from the system. Furthermore, either interface displacements of the structure $\mathbf{d}_\Gamma^{\mathrm{S}}$ or the interface velocity on the fluid side $\mathbf{u}_\Gamma^{\mathrm{F}}$ can be eliminated from the system, based on the choice of master and slave side for the mortar coupling.

4.1. *Structure split*

Here, the fluid field is chosen to be the master side for mortar coupling, i.e. $\mathbf{C}_{\mathrm{S}} = \mathbf{D}$ and $\mathbf{C}_{\mathrm{F}} = \mathbf{M}$. Since the structure displacements at the interface can then be removed from the system of equations, this case is referred to as *structure split*. The Jacobian matrix $\mathbf{J}$ of the FSI system (3.28) becomes

$$\begin{bmatrix} \mathbf{S}_{\mathrm{II}} & \mathbf{S}_{\mathrm{I\Gamma}} & & & & \\ \mathbf{S}_{\Gamma\mathrm{I}} & \mathbf{S}_{\Gamma\Gamma} & & & & \mathbf{D}^{\mathrm{T}} \\ & & \mathbf{F}_{\mathrm{II}} & \mathbf{F}_{\mathrm{I\Gamma}} + \frac{\Delta t}{2}\mathbf{F}_{\mathrm{I\Gamma}}^{\mathrm{G}} & \mathbf{F}_{\mathrm{II}}^{\mathrm{G}} & \\ & & \mathbf{F}_{\Gamma\mathrm{I}} & \mathbf{F}_{\Gamma\Gamma} + \frac{\Delta t}{2}\mathbf{F}_{\Gamma\Gamma}^{\mathrm{G}} & \mathbf{F}_{\Gamma\mathrm{I}}^{\mathrm{G}} & -\mathbf{M}^{\mathrm{T}} \\ & & \mathbf{0} & \frac{\Delta t}{2}\mathbf{A}_{\mathrm{I\Gamma}} & \mathbf{A}_{\mathrm{II}} & \\ & \mathbf{D} & & -\frac{\Delta t}{2}\mathbf{M} & & \end{bmatrix}. \tag{4.1}$$

The vector of unknowns $\boldsymbol{\Delta}\mathbf{x}_i^{n+1}$ remains unaltered, whereas the right-hand side vector $\mathbf{f}_i^{n+1}$ is modified to

$$\mathbf{f}_i^{n+1} = \begin{bmatrix} \mathbf{f}_{\mathrm{I},i}^{\mathrm{S},n+1} \\ \mathbf{f}_{\Gamma,i}^{\mathrm{S},n+1} \\ \mathbf{f}_{\mathrm{I},i}^{\mathrm{F},n+1} \\ \mathbf{f}_{\Gamma,i}^{\mathrm{F},n+1} \\ \mathbf{0} \\ \mathbf{0} \end{bmatrix} + \chi(i)\,\Delta t \begin{bmatrix} \mathbf{0} \\ \mathbf{0} \\ \mathbf{F}_{\mathrm{I\Gamma}}^{\mathrm{G}}\mathbf{u}_\Gamma^{\mathrm{F},n} \\ \mathbf{F}_{\Gamma\Gamma}^{\mathrm{G}}\mathbf{u}_\Gamma^{\mathrm{F},n} \\ \mathbf{A}_{\mathrm{I\Gamma}}\mathbf{u}_\Gamma^{\mathrm{F},n} \\ \mathbf{M}\,\mathbf{u}_\Gamma^{\mathrm{F},n} \end{bmatrix}, \tag{4.2}$$

with $\chi(i)$ defined in (3.10).

In a first step, we condense the Lagrange multipliers $\boldsymbol{\lambda}_i^{n+1}$ from the vector of unknowns (3.30). They can later be recovered from the solution, but in general their values are of little importance for FSI computations. The second row of the block system of equations is multiplied by the transposed projection matrix $\mathbf{P}^{\mathrm{T}}$, defined in (3.22), from the left, is added to the fourth row and is thereafter removed from the system whose matrix reduces to

$$\begin{bmatrix} \mathbf{S}_{\mathrm{II}} & \mathbf{S}_{\mathrm{I\Gamma}} & & & \\ & & \mathbf{F}_{\mathrm{II}} & \mathbf{F}_{\mathrm{I\Gamma}} + \frac{\Delta t}{2}\mathbf{F}_{\mathrm{I\Gamma}}^{\mathrm{G}} & \mathbf{F}_{\mathrm{II}}^{\mathrm{G}} \\ \mathbf{P}^{\mathrm{T}}\mathbf{S}_{\Gamma\mathrm{I}} & \mathbf{P}^{\mathrm{T}}\mathbf{S}_{\Gamma\mathrm{I}} & \mathbf{F}_{\Gamma\mathrm{I}} & \mathbf{F}_{\Gamma\Gamma} + \frac{\Delta t}{2}\mathbf{F}_{\Gamma\Gamma}^{\mathrm{G}} & \mathbf{F}_{\Gamma\mathrm{I}}^{\mathrm{G}} \\ & & \mathbf{0} & \frac{\Delta t}{2}\mathbf{A}_{\mathrm{I\Gamma}} & \mathbf{A}_{\mathrm{II}} \\ & \mathbf{D} & & -\frac{\Delta t}{2}\mathbf{M} & \end{bmatrix}. \tag{4.3}$$

The modification of the residual vector and the vector of the unknowns is straightforward

and is omitted here. For the applicability of the proposed approach it is important to note that the projection operator $\mathbf{P}$ and its transpose can be evaluated very efficiently due to the diagonal form of matrix $\mathbf{D}$.

For further simplification of the system (4.3), Eq. (3.27) is solved for the increment $\boldsymbol{\Delta}\mathbf{d}_{\Gamma,i}^{\mathrm{S},n+1}$ resulting in

$$\boldsymbol{\Delta}\mathbf{d}_{\Gamma,i}^{\mathrm{S},n+1} = \begin{cases} \Delta t \mathbf{P} \left(\frac{1}{2} \boldsymbol{\Delta}\mathbf{u}_{\Gamma,i}^{\mathrm{F},n+1} + \mathbf{u}_{\Gamma}^{\mathrm{F},n} \right), & i = 0 \\ \frac{\Delta t}{2} \mathbf{P}\, \boldsymbol{\Delta}\mathbf{u}_{\Gamma,i}^{\mathrm{F},n+1}, & i > 0 \end{cases} . \tag{4.4}$$

Substitution in system (4.3) yields the final Jacobian system $\tilde{\mathbf{J}} \tilde{\boldsymbol{\Delta}\mathbf{x}}_i^{n+1} = \tilde{\mathbf{f}}_i^{n+1}$ in which only fluid velocities have to be solved for at the interface. The block system matrix $\tilde{\mathbf{J}}$ can be written after reordering as

$$\begin{bmatrix} \mathbf{S}_{\mathrm{II}} & \frac{\Delta t}{2}\mathbf{S}_{\mathrm{I\Gamma}}\mathbf{P} & & \\ \mathbf{P}^{\mathrm{T}}\mathbf{S}_{\Gamma\mathrm{I}} & \frac{\Delta t}{2}\mathbf{P}^{\mathrm{T}}\mathbf{S}_{\Gamma\mathrm{I}}\mathbf{P} + \mathbf{F}_{\Gamma\Gamma} + \frac{\Delta t}{2}\mathbf{F}_{\Gamma\Gamma}^{\mathrm{G}} & \mathbf{F}_{\Gamma\mathrm{I}} & \mathbf{F}_{\Gamma\mathrm{I}}^{\mathrm{G}} \\ & \mathbf{F}_{\mathrm{I\Gamma}} + \frac{\Delta t}{2}\mathbf{F}_{\mathrm{I\Gamma}}^{\mathrm{G}} & \mathbf{F}_{\mathrm{II}} & \mathbf{F}_{\mathrm{II}}^{\mathrm{G}} \\ & \frac{\Delta t}{2}\mathbf{A}_{\mathrm{I\Gamma}} & \mathbf{0} & \mathbf{A}_{\mathrm{II}} \end{bmatrix}, \tag{4.5}$$

the modified vector of unknowns as

$$\tilde{\boldsymbol{\Delta}\mathbf{x}}_i^{n+1} = \begin{bmatrix} \boldsymbol{\Delta}\mathbf{d}_{\mathrm{I},i}^{\mathrm{S},n+1} \\ \boldsymbol{\Delta}\mathbf{u}_{\Gamma,i}^{\mathrm{F},n+1} \\ \boldsymbol{\Delta}\mathbf{u}_{\mathrm{I},i}^{\mathrm{F},n+1} \\ \boldsymbol{\Delta}\mathbf{d}_{\mathrm{I},i}^{\mathrm{G},n+1} \end{bmatrix} \tag{4.6}$$

and, finally, the modified residual as

$$\begin{aligned} \tilde{\mathbf{f}}_i^{n+1} = & \begin{bmatrix} \mathbf{f}_{\mathrm{I},i}^{\mathrm{S},n+1} \\ \mathbf{f}_{\Gamma,i}^{\mathrm{F},n+1} + \mathbf{P}^{\mathrm{T}}\mathbf{f}_{\Gamma,i}^{\mathrm{S},n+1} \\ \mathbf{f}_{\mathrm{I},i}^{\mathrm{F},n+1} \\ \mathbf{0} \end{bmatrix} \\ & + \chi(i)\, \Delta t \begin{bmatrix} \mathbf{S}_{\mathrm{I\Gamma}}\mathbf{P}\, \mathbf{u}_{\Gamma}^{\mathrm{F},n} \\ \left(\mathbf{P}^{\mathrm{T}}\mathbf{S}_{\Gamma\Gamma}\mathbf{P} + \mathbf{F}_{\Gamma\Gamma}^{\mathrm{G}}\right) \mathbf{u}_{\Gamma}^{\mathrm{F},n} \\ \mathbf{F}_{\mathrm{I\Gamma}}^{\mathrm{G}}\mathbf{u}_{\Gamma}^{\mathrm{F},n} \\ \mathbf{A}_{\mathrm{I\Gamma}}\mathbf{u}_{\Gamma}^{\mathrm{F},n} \end{bmatrix} . \end{aligned} \tag{4.7}$$

As it has been pointed out in Sec. 3.3.1 the case of conforming meshes implies an identity projection operator $\mathbf{P} = \mathbf{I}$, which maps between degrees of freedom on the fluid side and degrees of freedom on the structure side of the interface. Formally neglecting this transformation between the fields, the same monolithic FSI system is obtained as in [1] for the conforming case.

Note that in the non-conforming case the matrix products have to be carried out explicitly to obtain a suitable block matrix that can be handed to the linear solver.

4.2. *Fluid split*

Of course it is also possible to define the field of Lagrange multipliers $\boldsymbol{\lambda}$ on the fluid side, yielding $\mathbf{C}_{\mathrm{S}} = \mathbf{M}$ and $\mathbf{C}_{\mathrm{F}} = \mathbf{D}$. This approach is called *fluid split*, since there will be no velocity unknowns to be solved for at the fluid side of the interface. We obtain a Jacobian

matrix

$$\mathbf{J} = \begin{bmatrix} \mathbf{S}_{\mathrm{II}} & \mathbf{S}_{\mathrm{I}\Gamma} & & & & \\ \mathbf{S}_{\Gamma\mathrm{I}} & \mathbf{S}_{\Gamma\Gamma} & & & & \mathbf{M}^{\mathrm{T}} \\ & & \mathbf{F}_{\mathrm{II}} & \mathbf{F}_{\mathrm{I}\Gamma} + \frac{\Delta t}{2}\mathbf{F}^{\mathrm{G}}_{\mathrm{I}\Gamma} & \mathbf{F}^{\mathrm{G}}_{\mathrm{II}} & \\ & & \mathbf{F}_{\Gamma\mathrm{I}} & \mathbf{F}_{\Gamma\Gamma} + \frac{\Delta t}{2}\mathbf{F}^{\mathrm{G}}_{\Gamma\Gamma} & \mathbf{F}^{\mathrm{G}}_{\Gamma\mathrm{I}} & -\mathbf{D}^{\mathrm{T}} \\ & & \mathbf{0} & \frac{\Delta t}{2}\mathbf{A}_{\mathrm{I}\Gamma} & \mathbf{A}_{\mathrm{II}} & \\ & \mathbf{M} & & -\frac{\Delta t}{2}\mathbf{D} & & \end{bmatrix}. \tag{4.8}$$

Furthermore, the specific form of the FSI residual vector reads

$$\mathbf{f}_i^{n+1} = \begin{bmatrix} \mathbf{f}^{\mathrm{S},n+1}_{\mathrm{I},i} \\ \mathbf{f}^{\mathrm{S},n+1}_{\Gamma,i} \\ \mathbf{f}^{\mathrm{F},n+1}_{\mathrm{I},i} \\ \mathbf{f}^{\mathrm{F},n+1}_{\Gamma,i} \\ \mathbf{0} \\ \mathbf{0} \end{bmatrix} + \chi(i)\,\Delta t \begin{bmatrix} \mathbf{0} \\ \mathbf{0} \\ \mathbf{F}^{\mathrm{G}}_{\mathrm{I}\Gamma}\mathbf{u}^{\mathrm{F},n}_{\Gamma} \\ \mathbf{F}^{\mathrm{G}}_{\Gamma\Gamma}\mathbf{u}^{\mathrm{F},n}_{\Gamma} \\ \mathbf{A}_{\mathrm{I}\Gamma}\mathbf{u}^{\mathrm{F},n}_{\Gamma} \\ \mathbf{D}\,\mathbf{u}^{\mathrm{F},n}_{\Gamma} \end{bmatrix}, \tag{4.9}$$

where $\chi(i)$ is defined in (3.10). As before we only concentrate on the representation of the block system matrix and state the final representation of the vector of unknowns and residual vector at the end of the paragraph.

We proceed by eliminating the Lagrange multipliers $\boldsymbol{\lambda}$ from the system. Therefore the blocks in the fourth row are multiplied by $\mathbf{P}^{\mathrm{T}}$ from the left and then added to the second row of the block system. This yields a reduced 5-by-5 block system with system matrix

$$\begin{bmatrix} \mathbf{S}_{\mathrm{II}} & \mathbf{S}_{\mathrm{I}\Gamma} & & & \\ \mathbf{S}_{\Gamma\mathrm{I}} & \mathbf{S}_{\Gamma\Gamma} & \mathbf{P}^{\mathrm{T}}\mathbf{F}_{\Gamma\mathrm{I}} & \mathbf{P}^{\mathrm{T}}\left(\mathbf{F}_{\Gamma\Gamma} + \frac{\Delta t}{2}\mathbf{F}^{\mathrm{G}}_{\Gamma\Gamma}\right) & \mathbf{P}^{\mathrm{T}}\mathbf{F}^{\mathrm{G}}_{\Gamma\mathrm{I}} \\ & & \mathbf{F}_{\mathrm{II}} & \mathbf{F}_{\mathrm{I}\Gamma} + \frac{\Delta t}{2}\mathbf{F}^{\mathrm{G}}_{\mathrm{I}\Gamma} & \mathbf{F}^{\mathrm{G}}_{\mathrm{II}} \\ & & \mathbf{0} & \frac{\Delta t}{2}\mathbf{A}_{\mathrm{I}\Gamma} & \mathbf{A}_{\mathrm{II}} \\ & \mathbf{M} & & -\frac{\Delta t}{2}\mathbf{D} & \end{bmatrix}. \tag{4.10}$$

The last row of the system matrix is a representation of (3.27) and to remove it from the system we solve this equation for the fluid velocities $\mathbf{u}^{\mathrm{F},n+1}_{\Gamma,i}$ yielding

$$\boldsymbol{\Delta}\mathbf{u}^{\mathrm{F},n+1}_{\Gamma,i} = \begin{cases} \frac{2}{\Delta t}\mathbf{P}\boldsymbol{\Delta}\mathbf{d}^{\mathrm{S},n+1}_{\Gamma,i} - 2\mathbf{u}^{\mathrm{F},n}_{\Gamma}, & i = 0 \\ \frac{2}{\Delta t}\mathbf{P}\,\boldsymbol{\Delta}\mathbf{d}^{\mathrm{S},n+1}_{\Gamma,i}, & i > 0 \end{cases}, \tag{4.11}$$

which can thus be substituted in terms of the structure displacement. The reduced system matrix $\hat{\mathbf{J}}$ of the Jacobian $\hat{\mathbf{J}}\hat{\boldsymbol{\Delta}\mathbf{x}}_i^{n+1} = \hat{\mathbf{f}}_i^{n+1}$ is then given by

$$\begin{bmatrix} \mathbf{S}_{\mathrm{II}} & \mathbf{S}_{\mathrm{I}\Gamma} & & \\ \mathbf{S}_{\Gamma\mathrm{I}} & \mathbf{S}_{\Gamma\Gamma} + \mathbf{P}^{\mathrm{T}}\left(\frac{2}{\Delta t}\mathbf{F}_{\Gamma\Gamma} + \mathbf{F}^{\mathrm{G}}_{\Gamma\Gamma}\right)\mathbf{P} & \mathbf{P}^{\mathrm{T}}\mathbf{F}_{\Gamma\mathrm{I}} & \mathbf{P}^{\mathrm{T}}\mathbf{F}^{\mathrm{G}}_{\Gamma\mathrm{I}} \\ & \left(\frac{2}{\Delta t}\mathbf{F}_{\mathrm{I}\Gamma} + \mathbf{F}^{\mathrm{G}}_{\mathrm{II}}\right)\mathbf{P} & \mathbf{F}_{\mathrm{II}} & \mathbf{F}^{\mathrm{G}}_{\mathrm{II}} \\ & \mathbf{A}_{\mathrm{I}\Gamma}\mathbf{P} & \mathbf{0} & \mathbf{A}_{\mathrm{II}} \end{bmatrix}, \tag{4.12}$$

corresponding to a vector of unknowns

$$\hat{\boldsymbol{\Delta}\mathbf{x}}_i^{n+1} = \begin{bmatrix} \boldsymbol{\Delta}\mathbf{d}^{\mathrm{S},n+1}_{\mathrm{I},i} \\ \boldsymbol{\Delta}\mathbf{d}^{\mathrm{S},n+1}_{\Gamma,i} \\ \boldsymbol{\Delta}\mathbf{u}^{\mathrm{F},n+1}_{\mathrm{I},i} \\ \boldsymbol{\Delta}\mathbf{d}^{\mathrm{G},n+1}_{\mathrm{I},i} \end{bmatrix}, \tag{4.13}$$

containing only structure degrees of freedom at the interface. To complete the final linear system, the modified residual vector reads

$$\hat{\mathbf{f}}_i^{n+1} = \begin{bmatrix} \mathbf{f}_{\mathrm{I},i}^{\mathrm{S},n+1} \\ \mathbf{f}_{\Gamma,i}^{\mathrm{S},n+1} + \mathbf{P}^{\mathrm{T}} \mathbf{f}_{\Gamma,i}^{\mathrm{F},n+1} \\ \mathbf{f}_{\mathrm{I},i}^{\mathrm{F},n+1} \\ \mathbf{0} \end{bmatrix} + 2\,\chi(i) \begin{bmatrix} \mathbf{0} \\ \mathbf{P}^{\mathrm{T}} \mathbf{F}_{\Gamma\Gamma} \mathbf{u}_{\Gamma}^{\mathrm{F},n} \\ \mathbf{F}_{\mathrm{I}\Gamma} \mathbf{u}_{\Gamma}^{\mathrm{F},n} \\ \mathbf{0} \end{bmatrix}. \tag{4.14}$$

5. Concluding remarks

During this research the group from University of Colorado has been able to successfully understand the dual mortar method as it applies to incompressible FSI problems. Likewise, the research group from Technische Universität München has learned how non-linear surface effects such as wear can be used in an ALE formulation. We have successfully identified the hurdles to overcome in order to extend the dual mortar method to include compressible Navier-Stokes equations with non-linear fluid-thermal coupling. There is still work to be done to figure out the solutions to these hurdles and whether or not those solutions will be computationally prohibitive for implementation.

Acknowledgments

We would like to acknowledge and thank the Technische Universität München under summer program SBF/TRR 40 for organizing and funding this research collaboration.

References

[1] GEE, M. W., KÜTTLER, U. AND WALL, W. A. (2011). Truly monolithic algebraic multigrid for fluid-structure interaction. *Int. J. Numer. Meth. Engng*, **85**(8), 987–1016.

[2] BERNARDI, C., MADAY, Y. AND PATERA, A. T. (1994). A new nonconforming approach to domain decomposition: the mortar element method. In: Brezis, H. and Lions, J. L. (Eds.), *Nonlinear partial differential equations and their applications*, 13–51. Pitman/Wiley, London/New York.

[3] POPP, A., GEE, M. W. AND WALL, W. A. (2009). A finite deformation mortar contact formulation using a primal-dual active set strategy. *Int. J. Numer. Meth. Engng*, **79**(11), 1354–1391.

[4] POPP, A., GITTERLE, M., GEE, M. W. AND WALL, W. A. (2010). A dual mortar approach for 3D finite deformation contact with consistent linearization. *Int. J. Numer. Meth. Engng*, **83**(11), 1428–1465.

[5] PUSO, M. A. AND LAURSEN, T. A. (2004). A mortar segment-to-segment contact method for large deformation solid mechanics. *Comput. Methods Appl. Mech. Engrg.*, **193**(6-8), 601–629.

[6] PUSO, M. A. AND LAURSEN, T. A. (2004). A mortar segment-to-segment frictional contact method for large deformations. *Comput. Methods Appl. Mech. Engrg.*, **193**(45-47), 4891–4913.

[7] LAURSEN, T. A., PUSO, M. A. AND SANDERS, J. (2010). Mortar contact formulations for deformable-deformable contact: past contributions and new extensions for enriched and embedded interface formulations. *Comput. Methods Appl. Mech. Engrg.*, DOI:10.1016/j.cma.2010.09.006.

[8] FLEMISCH, B. AND WOHLMUTH, B. I. (2007). Stable lagrange multipliers for quadrilateral meshes of curved interfaces in 3D. *Comput. Methods Appl. Mech. Engrg.*, **196**(8), 1589–1602.

[9] PUSO, M. A. (2004). A 3D mortar method for solid mechanics. *Int. J. Numer. Meth. Engng*, **59**(3), 315–336.

[10] WOHLMUTH, B. I. (2000). A mortar finite element method using dual spaces for the Lagrange multiplier. *SIAM J. Numer. Anal.*, **38**(3), 989–1012.

[11] WOHLMUTH, B. I. (2001). *Discretization methods and iterative solvers based on domain decomposition*. Springer-Verlag, Berlin Heidelberg.

[12] LAMICHHANE, B. P., STEVENSON, R. P. AND WOHLMUTH, B. I. (2005). Higher order mortar finite element methods in 3D with dual Lagrange multiplier bases. *Numer. Math.*, **102**(1), 93–121.

[13] FÖRSTER, C., WALL, W. A. AND RAMM, E. (2009). Stabilized finite element formulation for incompressible flow on distorted meshes. *Int. J. Numer. Meth. Fluids*, **60**(10), 1103–1126.

[14] DONEA, J. AND HUERTA, A. (2003). *Finite Element Methods for Flow Problems*. Wiley, New York.

[15] HUGHES, T. J. R., SCOVAZZI, G. AND FRANCA, L. P. (2004). *Encyclopedia Of Computational Mechanics, Volume 3: Fluids*, chapter Multiscale and Stabilized Methods, 5–59. John Wiley & Sons, Ltd, Chichester.

[16] BRAESS, H. AND WRIGGERS, P. (2000). Arbitrary lagrangian eulerian finite element analysis of free surface flow. *Comput. Methods Appl. Mech. Engrg.*, **190**(1-2), 95–109.

[17] FERNANDEZ, M. A. AND MOUBACHIR, M. (2005). A newton method using exact jacobians for solving fluid-structure coupling. *Comput. Struct.*, **83**(2-3), 127–142.

[18] BISCHOFF, M., WALL, W. A., BLETZINGER, K.-U. AND RAMM, E. (2004). *Encyclopedia Of Computational Mechanics, Volume 2: Solids and Structures*, chapter Models and Finite Elements for Thin-walled Structures, 59–137. John Wiley & Sons, Ltd, Chichester.

[19] HUGHES, T. J. R. (1981). *The Finite Element Method - Linear Static and Dynamic Finite Element Analysis*. Dover Publications, New York.

[20] CHUNG, J. AND HULBERT, G. M. (1993). A time integration algorithm for structural dynamics with improved numerical dissipation: the generalized-alpha method. *J. Appl. Mech.*, **60**, 371–375.

[21] HÜEBER, S. AND WOHLMUTH, B.I. (2005). A primal-dual active set strategy for non-linear multibody contact problems. *Comput. Methods Appl. Mech. Engrg.*, **194**(27-29), 3147–3166.

[22] HARTMANN, S., BRUNSSEN, S., RAMM, E. AND WOHLMUTH, B. (2007). Unilateral non-linear dynamic contact of thin-walled structures using a primal-dual active set strategy. *Int. J. Numer. Meth. Engng*, **70**(8), 883–912.

[23] FARHAT, C., LESOINNE, M. AND LE TALLEC, P. (1998). Load and motion transfer algorithms for fluid/structure interaction problems with non-matching discrete interfaces: Momentum and energy conservation, optimal discretization and application to aeroelasticity. *Comput. Methods Appl. Mech. Engrg.*, **157**(1-2), 95–114.